

# **A Recoil Resilient Luminal Support**

by

**Arash Mehdizadeh**

B. Sc. (Computer Systems Engineering, Honours)  
Amirkabir University of Technology (Tehran Polytechnic), Iran, 2005

M. Sc. (Computer Architecture Engineering, First Class)  
Amirkabir University of Technology (Tehran Polytechnic), Iran, 2008

Thesis submitted for the degree of

**Doctor of Philosophy**

in

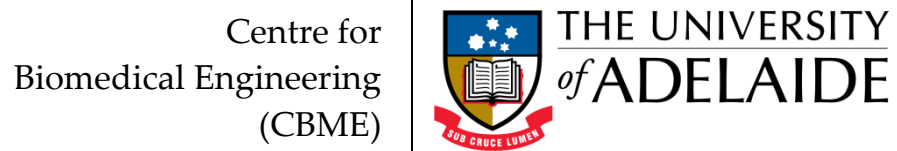
School of Electrical & Electronic Engineering  
Faculty of Engineering, Computer & Mathematical Sciences  
The University of Adelaide, Australia

April 2014

## Supervisors:

Dr Said Al-Sarawi, School of Electrical & Electronic Engineering

Prof. Derek Abbott, School of Electrical & Electronic Engineering



© 2014

Arash Mehdizadeh

All Rights Reserved

# Contents



<b>Contents</b> .....	<b>i</b>
<b>Abstract</b> .....	<b>v</b>
<b>Statement of Originality</b> .....	<b>ix</b>
<b>Acknowledgments</b> .....	<b>xi</b>
<b>Conventions</b> .....	<b>xv</b>
<b>Publications &amp; Awards</b> .....	<b>xvii</b>
<b>List of Symbols</b> .....	<b>xix</b>
<b>Abbreviations</b> .....	<b>xxv</b>
<b>List of Figures</b> .....	<b>xxvii</b>
<b>List of Tables</b> .....	<b>xxxi</b>
<b>Chapter 1. Introduction and Motivation</b> .....	<b>1</b>
1.1 Abstract.....	2
1.2 Atherosclerosis and Luminal Occlusion .....	3
1.3 Non-surgical Treatments .....	5
1.4 Surgical Treatments .....	6
1.4.1 Coronary Artery Bypass Grafting.....	6
1.4.2 Endarterectomy .....	7
1.4.3 Percutaneous Transluminal Angioplasty .....	8
1.4.4 Stenting.....	9
1.4.5 Atherectomy.....	11
1.5 Stents Current Status and the Future .....	13
1.5.1 Materials and Expansion Mechanism .....	15
1.5.2 Material Form.....	19

1.5.3 Fabrication Method.....	20
1.5.4 Design and Geometrical Features.....	23
I. Coil Stents.....	23
II. Spiral Stents.....	24
III. Woven Stents.....	25
IV. Modular (sequential) Stents.....	25
1.5.5 Stent Coatings and Surface Treatments.....	29
1.5.6 Stenting Limitations and Mitigation Efforts.....	31
I. Stent Recoil.....	31
I. Stent Thrombosis.....	32
II. Restenosis.....	33
1.6 Chapter Summary.....	35
1.7 Thesis Overview.....	37
1.7.1 Thesis Structure and Original Contributions.....	37
<b>Chapter 2. A Recoil Resilient Luminal Support.....</b>	<b>41</b>
2.1 Abstract.....	42
2.2 Introduction.....	43
2.3 Design and Modelling.....	47
2.3.1 Free Expansion Analysis.....	47
I. Materials and Methods.....	47
II. Results.....	51
2.3.2 Radial Strength.....	52
2.3.3 Axial Strength and Feasible Improvements.....	54
2.4 Fabrication.....	60
2.4.1 Machining.....	60
2.4.2 Shaping.....	61
I. Surface Profile.....	62
II. RRR Patency.....	63

2.4.3 Experimental Results.....	64
2.5 Chapter Summary.....	69
<b>Chapter 3. Hemodynamic Risk Assessment by Computational Fluid Dynamics .....</b>	<b>71</b>
3.1 Abstract.....	72
3.2 Introduction .....	73
3.3 Materials and Methods.....	75
3.3.1 Models Development .....	78
3.3.2 Discretisation.....	79
3.3.3 Dimensional Analysis.....	81
3.4 Results and Discussion.....	83
3.4.1 Part 1 – Unbranched Fluid Domain.....	83
I. LWSS in Unbranched Fluid Domains.....	83
II. Drag Force in the Unbranched Domains.....	92
3.4.2 Part 2 – Branched Fluid Domain.....	94
I. LWSS in Branched Fluid Domains.....	94
II. Drag Force and Output Flow Rate .....	96
3.4.3 Part 3 – Dimensional Analysis .....	103
I. Dimensional Assumptions and LWSS.....	104
II. Dimensional Assumptions, Drag Force and Flow Supply.....	106
III. Dimensional Assumptions, Final Notes.....	112
3.5 Chapter Summary.....	113
<b>Chapter 4. Thermal Actuation of the Recoil Resilient Ring.....</b>	<b>117</b>
4.1 Abstract.....	118
4.2 Introduction .....	118
4.3 Materials and Methods.....	121
4.4 Theoretical Analysis.....	124
4.4.1 Results .....	134
4.5 Numerical Analysis: Uniform Heat Transfer.....	136

4.5.1 Materials and Methods.....	137
4.5.2 Results.....	139
4.6 Numerical Analysis: Conjugate Heat Transfer .....	143
4.6.1 Materials and Methods.....	143
4.6.2 Results.....	147
4.7 Experimental Results .....	154
4.7.1 Heat-induced Actuation <i>in vitro</i> .....	157
4.7.2 Heat-induced Actuation in Free Expansion .....	158
4.7.3 Heat-induced Actuation Force .....	160
4.8 Electro-Thermal Actuation.....	164
4.8.1 Theoretical Framework .....	165
4.8.2 Numerical Analysis.....	169
I. Materials and Methods .....	169
II. Results.....	172
4.9 Chapter Summary .....	176
<b>Chapter 5. Conclusion and Future Directions.....</b>	<b>179</b>
5.1 Introduction.....	180
5.2 Contributions and Conclusions.....	181
5.3 Recommendations for Future Work .....	187
5.4 Closing Comments.....	188
<b>Bibliography.....</b>	<b>189</b>
<b>Index.....</b>	<b>209</b>
<b>Biography.....</b>	<b>215</b>
<b>Scientific Genealogy .....</b>	<b>216</b>

# Abstract



Cardiovascular disease (CVD) refers to a class of diseases affecting normal function of cardiovascular system and its momentous role to carry oxygenated blood to the entire body. Taking lives of more than 17 million people in 2008, CVD has yet remained as the primary cause of deaths around the world. Statistics from World Health Organisation in 2002 associated CVD with 10% of the disability-adjusted life years lost in low/middle-income countries and 18% in high-income countries.

Atherosclerosis, as one of the primary causes of CVD, refers to the thickening of vascular walls due to deposition of fatty materials wherein it can lead to impeded or completely occluded blood flow. Obstruction of coronary arteries, referred to as coronary heart disease (CHD), is estimated to become the single leading health problem by 2020. Occurrence and further development of CHD is associated with a number of biological and environmental factors such as an individual's genetic predisposition, lifestyle, climate conditions, exercise habits and emotions to name a few.

Treatment and management of vascular constrictions consists of a combination of non-surgical and surgical methods. The former includes approaches such as healthy lifestyle changes and pharmacological interventions while the later includes bypass grafting, balloon angioplasty with or without deployment of a stent and atherectomy. Stents are mechanical devices that provide a chronic support against internal walls of occluded vessels to restore their normal luminal patency. In the past decade, stenting has prevailed as the conventional treatment option in management of CVD, exceeding current number of bypass grafting procedures, owing this success to its proven efficacy in short and long-term treatment of occluded vessels. Common stent structures are simply made of a metal mesh, e.g. stainless steel, and deployed in a blood vessel such as an artery during a percutaneous coronary intervention procedure, also known as angioplasty. Several attempts to meet the often self-competing objectives of stents such as high radial strength, low elastic recoil, axial flexibility, trackability in tortuous paths, biocompatibility and radio-

capacity gave birth to a multitude of different stent design and improvement iterations to date. The acute luminal gain after stenting is often compromised by the two most common post intervention complications, namely in-stent thrombosis (formation of blood clot) and restenosis (re-narrowing of the lesion). Induced trauma during stent deployment is proven to play a key role in the occurrence of these complications. Elastic recoil of stents after deployment due to the intrinsic material properties and the compressive forces from a vessel accounts for both acute and chronic luminal loss after stent deployment. Mitigation measures such as over-expansion in balloon-expandable (BE) stents and use of self-expandable (SE) stents so far have proven to aggravate vascular trauma leading to thrombosis and restenosis. Pharmacological approaches such as systemic administration of blood-thinners or localized drug release in drug-eluting (DE) stents aim to control these complications by inhibition of an accentuated inflammatory response from the body. Despite the promising results in reduction of restenosis after use of DE stents, increased rate of late thrombosis raised concerns about efficacy of these stents in comparison with bare-metal (BM) stents. Moreover, it is important to note that in these approaches the mechanical aspect of the problem still stands. As a result, to meet the often-competing aforementioned imperatives of stents, a new design paradigm is called for.

To address the issue of recoil and extend capability of current stents to controlled and incremental expansion steps with alternative expansion mechanisms, in this thesis a novel recoil resilient stent is proposed and developed. The proposed luminal support called a recoil resilient ring (RRR) is an open ring with overlapping ends and asymmetrical sawtooth structures from the two ends that are intermeshed. Utilized as a standalone support or integrated with other stent structures, upon expansion of the RRR, the teeth from opposite ends can slide on top of each other, yet interlock step-by-step in the opposite direction so to keep the final expanded state against compressive forces that normally cause recoil.

Design, fabrication and compatibility of the proposed stent with current state-of-the-art stent deployment procedures and its superior radial strength in comparison with commercial stents are extensively studied in this thesis through finite element modelling (FEM) and experimental studies. The RRR is fabricated from Nitinol sheets with transformation temperatures well above typical body temperature ensuring martensite mode



of operation of the device after deployment. Fabrication is carried out by linear patterning of Nitinol sheets of 200- $\mu\text{m}$  thickness utilizing  $\mu\text{EDM}$  technology. Superior radial strength of the RRR in comparison with a commercial stent composed of the stiffer material, stainless steel, is demonstrated via experimental and numerical studies.

Hemodynamic risk assessment of the proposed design as a standalone and integrated support compared with a typical commercial stent is then carried out by transient computational fluid dynamics (CFD). Subject to a realistic pulsatile blood flow, spatial and temporal restenosis risk indicators of three luminal supports are extensively studied utilizing CFD. These luminal supports include a standalone RRR, a nominal BE stent and an RRR-integrated stent. Risk factors including extension of areas subject to low wall shear stress as the primary risk factor of restenosis after deployment, tendency of supports to migrate in response to fluid drag forces as well as flow supply changes to side branches are extensively investigated. Furthermore, sensitivity of the results to the dimensional assumptions of the deployment domain, branching vessels and patency of the supports is studied. Our results indicate superior hemodynamic performance of the standalone RRR compared with the others. In addition, close correspondence of the performance indicators of RRR-integrated stent and the standalone stent demonstrates minimal hemodynamic footprint of the proposed RRR highlighting its merit as a viable luminal support given its superior radial strength.

Attractive attributes such as shape memory effect of Nitinol, the thermally trained expanded shape of the RRR, its unique incremental slide and lock expansion mechanism and its higher transformation temperature compared to the body temperature, bring new potential for alternative controlled and incremental actuation of the RRR. These alternative expansion methods, by application of direct or electrically-induced heat are further explored through extensive analytical, multi-field numerical and experimental studies. The knowledge and contributions made in the current work, in addition to the design, development, experimental and multi-field numerical results provide a general engineering framework applicable to other biomedical luminal supports in the future.

This page is left blank intentionally

# Statement of Originality



This work contains no material that has been accepted for the award of any other degree or diploma in any university or other tertiary institution and, to the best of my knowledge and belief, contains no material previously published written by another person, except where due reference has been made in the text.

I give consent to this copy of my thesis, when deposited in the University Library, being made available for loan and photocopying, subject to the provisions of the Copyright Act 1968.

I also give permission for the digital version of my thesis to be made available on the web via the University's digital research repository, the Library catalogue, the Australasian Digital Thesis Program (ADTP) and also through web search engines, unless permission has been granted by the University to restrict access for a period of time.

---

Signed

---

Date

This page is left blank intentionally

# Acknowledgments



Now that the multidisciplinary journey of this research has come to a conclusion, I truly understand the power of collaboration and its momentous role to realise the wildest of dreams. I am thrilled to have this opportunity to express my gratitude and acknowledgement to those around me, to only some of whom it is possible to give particular mention here. All the people who shed light on different aspects of my personal and academic life in this period undoubtedly deserve a big cheer.

First and foremost, I would like to express my sincerest gratitude to my principal supervisor **Dr Said Al-Sarawi** from the school of Electrical and Electronic Engineering at the University of Adelaide. His open mind and receptive attitude towards new ideas, taught me how to let ideas fly beyond boundaries and consider nothing as being off-limits. While continuously providing support to improve my critical thinking and make progress on the set milestones, every single meeting with Dr Al-Sarawi was an absolute joy. His investigative and progressive approach towards other branches of science gave me the drive to feed my curious mind and plunge into different disciplines such as biology, optimization, micro-electronics, and mechanical engineering all of which equipped me with the necessary skills to tackle the present work. He has been a genuine mentor to me on this journey and I sincerely thank him for that.

My special gratitude is extended to my co-supervisor **Prof. Derek Abbott** from the School of Electrical and Electronic Engineering at the University of Adelaide who laid the foundation for the commencement of my research at this university. Prof. Abbott's unsurpassed friendly, supportive and informative attitude was very apparent even before I met him in person. His initiative to provide guidance in administrative and collaborative efforts provided me with invaluable experiences and lessons that I will carry for the rest of my life. His meticulous and critical eye enriched the content of this thesis for which I am grateful.

Physical implementation of the proposed designs in this thesis could have not been realized without the support and extensive help of **Dr Kenichi Takahata** from the department of Electrical and Computer Engineering at the University of British Columbia (UBC), Vancouver, Canada. His venerated expertise on stents and MEMS research and his influential and supportive mentorship during my visit to Microsystems and Nanotechnology Group (MiNa) at UBC provided me with invaluable direction and technical support to accomplish key components of this research. Also, I would like to acknowledge the friendly and insightful advice that I have received from Prof. York Hsiang from Vascular Surgery Department at the University of British Columbia, Vancouver, Canada.

In this vein, I would like to extend my gratitude to my dear friends and colleagues in UBC who assisted me during this period to feel at home and part of a great scientific taskforce. I acknowledge help and support of (in a random order) Dr Mohamed Sultan Mohamed Ali for his assistance on fabrication of microdevices and his critical and technical reviews and enlightening suggestions, Dr Reza Rashidi for his critical yet encouraging support on development of stents, Mr Masoud Dahmardeh for being an incredible friend during my visit to Canada and his indispensable help on micromachining and physical evaluation of prototypes, and Mr Babak Assadsangabi for his insightful ideas on structural analysis of the proposed structures in COMSOL.

I would also like to convey my gratitude to The University of Adelaide for the funding and support provided for this research to make it a success. This project would have not been accomplished without the financial assistance via the international postgraduate scholarship (ASI) and travel grants including Research Abroad Scholarship, University of Adelaide and BUPA Postgraduate Travel Grant and AUGU/RC Heddle Award that facilitated my visit to UBC. I acknowledge the support and expertise of Mr Simon Doe and Mr Dapankar Chugh at Ian Wark Research Institute at the University of South Australia for providing access to optical profilometer. Numerical analysis has been an integral part of this thesis and I am pleased to thank the helpful support of Leap Australia, Australia and CMC Microsystems, Canada support teams for their guidance on finite element modelling packages ANSYS and COMSOL.

Constant support and help of the academic and professional staff at the School of Electrical and Electronic Engineering at the University of Adelaide, undeniably, deserves a special thanks. Especially, I would like to mention Mrs. Ivana Rebellato, Mrs. Rose-Marie Descalzi, Mr Stephen P. Guest and Mr Danny Di Giacomo form the administration team in addition to Mr David Bowler, Mr Mark Innes, Mr Greg Pullman and Mr Ryan King from IT and technical support for their unlimited support and patience with the multitude of requests that I had in this period. I also wish to express my thanks to Mr Ian Linke for his insightful technical suggestions and assistance for macro-fabrication of the first prototype. I also enjoyed being a proud member of our schools team in a number of athletic events to experience their cooperative spirit yet in another level.

I am deeply grateful to all my colleagues and good friends as they enriched my life during this journey by their motivational encouragement and helpful suggestions. Particularly, I wish to thank my dearest friends, who in fact have become my family in Australia, Mr Nikan Rostamzadeh Torghabeh and Dr Pawel Kuklik, for both their insightful directions into different theoretical aspects of my thesis and most importantly making life in Adelaide an unforgettable joy. I will always remember our countless hours of discussions, often turning into arguments, on subjects such as electromagnetism, fluid mechanics and even the cosmos that, albeit the following headaches and disagreements, challenged us constantly. My gratitude is extended especially to Nikan for his invaluable help and friendly dedication during our extensive discussions on fluid mechanics and computational fluid dynamics (CFD) that were indispensable to the accomplishment of this project.

Among my fellow postgraduate students, I would like to thank Dr Muammar Kabir for his kind help, valuable friendship and encouraging conversations that we had together, Dr Don W. Dissanayake for his expertise on biomedical implants and our fruitful discussions on pilot studies and Mr Shaoming Zhu, Mr Henry Ho and Dr Gretel M. Png for providing such a friendly and pleasant environment to work in.

## Acknowledgments

---

Above all, I would like to convey my endless appreciation to my family for their unconditional love, perpetual support and patience throughout my life. A special expression of gratitude goes to my dearest parents Shahnaz and Majid for the sacrifices they made in their lives to empower me become who I am today.

In the end I dedicate this thesis to my grandfathers whose vision for excellence reverberated through generations and beyond.

Arash Mehdizadeh



# Conventions



**Formatting:** For typesetting and image production of this thesis, Microsoft (MS) Office suite 2010 is used. Plots and images were generated using Matlab 10.0 (Mathworks Inc.) and MS Excel 2010.

**Spelling:** Australian English spelling is adopted, as defined by the Macquarie English Dictionary (Delbridge 2001).

**Referencing:** IEEE style is used for referencing and citations in this thesis managed by Endnote X6 (Thomson Reuters).

This page is left blank intentionally

# Publications & Awards



## Journal Articles

---

- **A. Mehdizadeh**, M. S. M. Ali, K. Takahata, S. Al-Sarawi, and D. Abbott, "A recoil resilient lumen support, design, fabrication and mechanical evaluation," *Journal of Micromechanics and Microengineering*, vol. 23, art. no. 065001, 2013.
- M. K. Kopaei, **A. Mehdizadeh**, D. C. Ranasinghe, and S. Al-Sarawi, "A novel hybrid approach for wireless powering of biomedical implants," *IEEE Sensors Journal*, 2013 (Submitted, Under Review).
- A. Mirsepahi, **A. Mehdizadeh**, L. Chen, and B. O'Neill, "A comparative approach between intelligent techniques and conventional methods for inverse heat transfer modelling of an irradiative dryer," *Journal of International Communications in Heat and Mass Transfer*, 2013 (Submitted).

## Conferences

---

- M. K. Kopaei, **A. Mehdizadeh**, D. C. Ranasinghe, and S. Al-Sarawi, "A novel hybrid approach for wireless powering of biomedical implants," in *2013 IEEE Eighth International Conference on Intelligent Sensors, Sensor Networks and Information Processing*, , 2013, pp. 455-460.
- **A. Mehdizadeh**, S. Al-Sarawi, K. Takahata, and D. Abbott, "A novel stent for recoil resilience," presented at *the Australian Biomedical Engineering Conference (ABEC)*, Brisbane, Queensland, 2012.
- **A. Mehdizadeh**, A. K. Horestani, S. F. Al-Sarawi, and D. Abbott, "An efficient 60 GHz resonator using Harmony Search," in *2011 IEEE Conference on Recent Advances in Intelligent Computational Systems (RAICS)*, 2011, pp. 369-372.
- **A. K. Horestani**, A. Mehdizadeh, S. Al-Sarawi, C. Fumeaux, and D. Abbott, "Quality factor optimization process of a tapered slow-wave coplanar strips resonator in CMOS technology," in *Microwave Conference Proceedings (APMC), 2011 Asia-Pacific*, 2011, pp. 45-48.

- **A. Mehdizadeh**, A. Miremadi, S. Al-Sarawi, M. Arjomandi, S. Mehdizadeh, B. Dally, and D. Abbott, "Optimal design of an offset strip fin heat sink using harmony search," in *38th Chemeca 2010: Engineering at the Edge*, Hilton Adelaide, South Australia, 2010, pp. 848-858.
- **A. Miremadi**, A. Mehdizadeh, M. Arjomandi, S. Al-Sarawi, M. Kahrom, B. Dally, and D. Abbott, "Taguchi based performance analysis or an offset strip fin heat sink," in *38th Chemeca 2010: Engineering at the Edge*, Hilton Adelaide, South Australia, 2010, pp. 1-10.

## Awards

---

- Young Biomedical Engineer Prize awarded by Engineers Australia at the 12<sup>th</sup> Australian Biomedical Engineering Conference (ABEC), Brisbane, Australia, 2012.
- Research Abroad Scholarship travel grant to visit Microsystems and Nanotechnology (MiNa) research group at the University of British Columbia (UBC), Vancouver, Canada, awarded by University of Adelaide, 2011.
- BUPA Postgraduate Travel Grant and AUGU/RC Heddle Award travel scholarship to visit Microsystems and Nanotechnology (MiNa) research group at the University of British Columbia (UBC), Vancouver, Canada, 2011.
- Selected runner for the 3-Minute thesis competition, Faculty of Engineering Computer Science & Mathematical Sciences, School of Electrical & Electronic Engineering, The University of Adelaide, 2010.
- Postgraduate research Scholarship (ASI) towards doctoral studies, The University of Adelaide, Nov 2008.

# List of Symbols



Notation	Description
$CSA_{pre}$	Luminal cross-sectional area before deflation of balloon
$CSA_{post}$	Luminal cross-sectional area after deflation of balloon
$\rho_0$	Initial density
$V_0$	Initial volume
$V(t)$	Current volume
$m_0$	Initial mass
$\rho$	Density
$t$	Time
$\sigma_{ij}$	Stress tensor component $ij$
$\ddot{x}$	Acceleration component in the $x$ direction
$\ddot{y}$	Acceleration component in the $y$ direction
$\ddot{z}$	Acceleration component in the $z$ direction
$b_i$	Body acceleration in the direction of axis $i$ .
$\varepsilon_{ij}$	Strain tensor component $ij$
$m$	Mass
$F$	Force
$\dot{x}_i$	Velocity in the $i$ direction
$\{x\}$	Nodal displacement vector
$[K]$	Stiffness matrix
$\{F\}$	Nodal force vector
$D_{effective}$	Effective internal diameter of a scaffold
$D_{dilated}$	Average external diameter of a scaffold
$D_{lost}$	Diameter loss due to strut thickness

Notation	Description
$T_s$	Strut thickness
$G_P$	Patency gain
$A_C$	Average cross-sectional area patent to fluid
$A_T$	Mean cross-sectional area of a deployed scaffold
$T_{s,avg}$	Average strut thickness
$T_{s,flat}$	Fabricated RRR thickness with no sawtooth
$t_h$	RRR sawtooth height
$t_l$	RRR sawtooth length
$O_l$	RRR overlap length
$R_l$	RRR total length
$\mathbf{V}$	Fluid velocity vector
$p$	Fluid pressure
$\mu$	Dynamic viscosity
$\mathbf{D}$	Rate of deformation tensor
$\mu_\infty$	Viscosity at zero shear rate
$\mu_0$	Viscosity at infinite shear rate
$\dot{\gamma}$	Shear rate
$u$	Velocity component in the direction of $x$ axis
$v$	Velocity component in the direction of $y$ axis
$w$	Velocity component in the direction of $z$ axis
$D_{in,avg}$	Mean inner diameter of a scaffold
$W_s$	Strut width
$T_s$	Strut thickness
$D_{in,m}$	Main vessel diameter
$D_{in,m}$	Branching vessel diameter
$L_{Prox,Stent}$	Boundary layer initial length, proximal end of stent
$L_{Dist,Stent}$	Boundary later initial length, distal end of stent
$L_{Prox,RRR-Stent}$	Boundary layer initial length, proximal end of RRR-stent
$L_{Dist,RRR-Stent}$	Boundary later initial length, distal end of RRR-stent

Notation	Description
$F_{wh}$	Scaffolding withholding force
$F_d$	Fluid drag force
$f_{i, support}$	Branch $i$ outlet flow rate, main branch scaffolded
$f_{in}$	Inlet flow rate
$FR_i$	Outlet/Inlet flow rate ratio
$f_{i, healthy}$	Branch $i$ outlet flow rate, main branch unscaffolded
$FD_i$	Outlet/Inlet flow rate ratio deviation
$A_{RRR-Stent}$	Area subject to low wall shear stress, RRR-stent
$A_{Stent}$	Area subject to low wall shear stress, stent
$A_s$	SMA starting transformation temperature
$A_f$	SMA finishing transformation temperature
$L_{sty,r}$	Axial length of Styrofoam rings
$L_{sty,c}$	Axial length of Styrofoam cap
$L_{rod}$	Axial length of heat transfer rod
$r_1$	Radius of heat transfer rod
$L_{air,r}$	Axial length of air cylinder trapped, Styrofoam rings
$L_{air,d}$	Axial length of air cylinder at the deployment area
$r_2$	Mock vessel internal diameter
$T_{sty,r}$	Thickness of Styrofoam rings
$L_{mock}$	Axial length of mock vessel
$L_{RRR}$	Total length of RRR
$t_{RRR}$	RRR average thickness
$W_{RRR}$	RRR width
$V_{flow}$	Approach velocity
$k_{rod}$	Thermal conductivity of heat transfer rod
$k_{sty}$	Thermal conductivity of Styrofoam
$k_{air}$	Thermal conductivity of air
$\nu$	Kinematic viscosity

Notation	Description
Re	Reynolds number
Pr	Prandtl number
$\dot{Q}$	Heat transfer rate
$T$	Temperature
$R_{\text{thermal}}$	Thermal resistance
$R_{\text{cond}}$	Conduction thermal resistance
$R_{\text{conv}}$	Convective thermal resistance
$h$	Convective heat transfer coefficient
$R_{\text{rad}}$	Radiation thermal resistance
$h_{\text{rad}}$	Radiation heat transfer coefficient
$T_s$	Surface temperature
$T_{\text{surr}}$	Surrounding temperature
$R_1 = R_{\text{cond\_ins}}$	Conductive thermal resistance of air and Styrofoam rings
$R_2 = R_{\text{cond\_mock}}$	Conductive thermal resistance of mock vessel
$R_3 = R_{\text{conv}}$	Convective thermal resistance of crossflow
$k_{\text{ins}}$	Thermal conductivity of insulation layer
Nu	Nusselt Number
$\dot{q}_{\text{conv}}$	Convective heat flux rate
$\dot{q}_{\text{cond}}$	Conductive heat flux rate
$h_{\text{flow}}$	Effective heat transfer coefficient of crossflow
$L_{\text{chr}}$	Characteristic length
$\text{Nu}_{\text{cyl}}$	Nusselt number of cylinder in crossflow
$T_1$	Temperature at internal walls of mock vessel
$T_{\infty 1}$	Constant rod temperature
$R_{\text{total}}$	Total thermal resistance
$\dot{Q}_{\text{in}}(x)$	Heat transfer rate into the differential volume at distance $x$
$\dot{Q}_{\text{out}}(x)$	Heat transfer rate out of the diff. volume at distance $x$
$\dot{Q}_{\text{comb}}(x)$	Heat transfer rate out of the diff. volume in radial direction
$R_{\text{comb}}$	Combined thermal resistance of insulation layer



Notation	Description
$A_c$	Cross-sectional area of heat transfer rod
$L_{\text{total}}$	Total length of the thermal model of heat transfer rod
$L_{\text{added}}$	Added length to the thermal mode of heat transfer rod
$\dot{Q}_{\text{out,tip}}$	Heat transfer rate from the tip of heat transfer rod
$x_{\text{tip}}$	Axial distance from base to tip of heat transfer rod
$\dot{Q}_{\text{added}}$	Heat transfer from added length of heat transfer rod
$T_{\text{rod}}(x)$	Temperature of rod at axial distance $x$ from the base
$R_{\text{total\_tip}}$	Total thermal resistance at the tip of the rod
$R_{\text{ins}}$	Thermal resistance of the insulation at the top section of mock-rod assembly
$A_{c,\text{ins}}$	Cross-sectional area of Styrofoam cap
$k_{\text{ins,top}}$	Thermal conductivity of insulation at the top section of mock-rod assembly
$h_{\text{top}}$	Heat transfer coefficient at the top of mock rod assembly
$R_{\text{top}}$	Thermal resistance at the top of mock-rod assembly
$L_{\text{top}}$	Axial length of the top section of the mock-rod assembly
$P_{\text{mock}}$	Periphery of the mock vessel
$A_{c,\text{mock}}$	Cross-sectional area of mock vessel
$\dot{p}$	Heat transfer rate per unit length
$R_{\text{mock}}$	Effective thermal resistance of mock vessel
$[K]$	Matrix of thermal conductance
$\dot{Q}_{\text{electric}}$	Electric power consumption
$I$	Electric current
$R_{\text{electric,plate}}$	Electrical resistance of heating plate
$\dot{Q}_{\text{thermal}}$	Thermal heat transfer rate
$R_{\text{thermal,plate}}$	Thermal resistance of heating plate
$T_{\text{plate}}$	Heating plate temperature
$T_{\text{room}}$	Room temperature

Notation	Description
$\delta_{\text{linear}}$	Coefficient of linear thermal expansion
$L_{\text{initial}}$	Initial length of a solid
$V_{\text{electric}}$	Electric potential
$I_{\text{electric}}$	Electric current
$T_{\text{RRR}}$	RRR body temperature
$T_{\text{body}}$	RRR's surrounding tissue (human body) temperature
$R_{\text{thrm,body}}$	Thermal resistance tissue surrounding RRR
$R_{\text{thrm,blood}}$	Effective thermal resistance of blood
$R_{\text{elec,RRR}}$	Electrical resistance of RRR
$V_{\text{in}}, V_{\text{out}}$	Input and output voltage
$R_{\text{cond,parylene}}$	Conduction thermal resistance of parylene
$R_{\text{conv,blood}}$	Convective thermal resistance of blood
$L_{\text{coating}}$	Thickness of parylene-C layer
$k_{\text{parylene}}$	Thermal conductivity of parylene
$A_{\text{RRR,conv}}$	RRR area subject to blood flow
$h_{\text{blood}}$	Convective heat transfer coefficient of blood
$\rho_{\text{elec,Nitinol}}$	Electrical resistance of Nitinol
$A_{\text{RRR,cs}}$	RRR strut cross-sectional area
$V_{\text{avg,blood}}$	Average blood velocity
$\rho_{\text{blood}}$	Blood density
$\mu_{\text{blood}}$	Average blood viscosity
$P_{\text{RRR}}$	Cross-sectional periphery of RRR
<b>f</b>	Fluid body forces

# Abbreviations



Notation	Description
$\mu$ EDM	Micro Electro-Discharge Machining
3D	Three-Dimensional
ACE	Angiotensin-Converting Enzyme
ARB	Angiotensin II Receptor Antagonist
BE	Balloon-Expandable
BM	Bare-Metal
CABG	Coronary Artery Bypass Grafting
CAD	Computer-Assisted Design
CFD	Computational Fluid Dynamics
CHD	Coronary Heart Disease
CNT	Carbon Nanotube
Co-Cr	Cobalt Chromium
CSA	Cross-Sectional Area
CTE	Coefficient of Thermal Expansion
CU	Copper
CVD	Cardiovascular Disease
DE	Drug-eluting
Fe	Iron
FEA	Finite Element Analysis
FEM	Finite Element Modelling
HT	Heat transfer Rod
IR	Infrared
ISR	In-Stent Restenosis
LDL	Low Density Lipoproteins
LWSS	Low Wall Shear Stress
Mg	Magnesium

Notation	Description
MRI	Magnetic Resonance Imaging
Ni-Ti	Nickel-Titanium (Nitinol)
PCI	Percutaneous Coronary Intervention
PCTA	Percutaneous Transluminal Angioplasty
PET	Polyethylene Terephthalate
PEVA	Polyethylene- <i>co</i> -Vinyl Acetate
PGA	Polyglycolid Acid
PLA	Polylactic Acid
PLGA	Poly- <i>l</i> -Glycolic Acid
PMBA	Poly- <i>n</i> -Butyl Methacrylate
Pt-Cr	Platinum Chromium
Pt-Ir	Platinum Iridium
PU	Polyurethane
RF	Radio-Frequency
RRR	Recoil Resilient Ring
SE	Self-Expandable
SIBS	Styrene- <i>b</i> -Isobutylene- <i>b</i> -Styrene
SMA	Shape Memory Alloy
SS 316L	Stainless Steel 316L
SST	Shear Stress Transport
STD	Standard Deviation
Ti	Titanium
TiBN	Titanium-Boron-Nitride
VLSI	Very Large Scale Integration

# List of Figures



<b>Chapter 1</b> .....	<b>1</b>
Figure 1.1 . Composition of arterial walls. ....	4
Figure 1.2 . Occurrence and growth of atherosclerosis. ....	5
Figure 1.3 . Coronary artery bypass grafting. ....	7
Figure 1.4 . Carotid artery endarterectomy. ....	8
Figure 1.5 . Percutaneous transluminal angioplasty (PCTA). ....	8
Figure 1.6 . Dissection after percutaneous coronary angioplasty. ....	9
Figure 1.7 . Balloon expansion of a coronary stent. ....	10
Figure 1.8 . Common atherectomy techniques. ....	12
Figure 1.9 . Stent classification map. ....	16
Figure 1.10 . Expansion of balloon and self-expandable stents. ....	17
Figure 1.11 . Coil stents. ....	24
Figure 1.12 . Spiral stents. ....	25
Figure 1.13 . Woven stents. ....	26
Figure 1.14 . Closed-cell modular stent. ....	26
Figure 1.15 . Stent with flexible bridges. ....	27
Figure 1.16 . Closed-cell stent with flexible bridges. ....	28
Figure 1.17 . Open cell modular stent. ....	28
Figure 1.18 . Fish scaling and plaque prolapse in open cell stents. ....	29
Figure 1.19 . Stent thrombosis in a DE stent. ....	32
Figure 1.20 . In-stent restenosis. ....	34
Figure 1.21 . Overview of thesis structure. ....	38
<b>Chapter 2</b> .....	<b>41</b>
Figure 2.1 . Recoil Resilient Ring (RRR) luminal support. ....	45
Figure 2.2 . Finite element model of the simplified RRR. ....	50
Figure 2.3 . Radial displacement and stress results during expansion. ....	51
Figure 2.4 . Plastic strain results of the teeth. ....	52

Figure 2.5 . BE stent resilience against compression. ....	53
Figure 2.6 . RRR resilience against compression. ....	54
Figure 2.7 . Computational model of RRR in axial loading analysis. ....	55
Figure 2.8 . Axial loading results of the RRR without axial support. ....	56
Figure 2.9 . Axial harnesses. ....	57
Figure 2.10 . Use of axial harnesses in the fully expanded state. ....	58
Figure 2.11 . Discretised 3D model of RRR with axial harnesses. ....	58
Figure 2.12 . Axial loading results of the RRR with axial harnesses. ....	59
Figure 2.13 . Plastic deformation of axial harnesses. ....	59
Figure 2.14 . Straight RRR, $\mu$ EDM patterned from a 200- $\mu$ m-thick Nitinol sheet. ....	60
Figure 2.15 . RRR shaping and thermal treatment setup. ....	61
Figure 2.16 . RRR after shaping and thermal treatment. ....	62
Figure 2.17 . Surface profile of RRR. ....	63
Figure 2.18 . Balloon expansion of RRR <i>in vitro</i> . ....	65
Figure 2.19 . Radial loading test setup. ....	66
Figure 2.20 . Radial loading test results, free-holding. ....	68
Figure 2.21 . Radial loading test results, <i>in vitro</i> . ....	69
<b>Chapter 3</b> .....	<b>71</b>
Figure 3.1 . Geometry of the three different supports. ....	77
Figure 3.2 . Fluid domain configurations of the CFD analysis. ....	79
Figure 3.3 . Inlet flow profile. ....	80
Figure 3.4 . Discretization of the fluid domain. ....	80
Figure 3.5 . Dimensional configurations of the dimensional analysis. ....	82
Figure 3.6 . LWSS distribution in unbranched fluid domains. ....	84
Figure 3.7 . Temporal average of LWSS in unbranched fluid domains. ....	84
Figure 3.8 . Selected time instances of third cardiac cycle. ....	85
Figure 3.9 . Inverse relation of the dynamic viscosity and shear rate, standalone stent. ....	86
Figure 3.10 . Inverse relation of the dynamic viscosity and shear rate, RRR-integrated stent. ....	86
Figure 3.11 . LWSS contour plots, deployment area of unbranched domains, instances 1–3. ....	87
Figure 3.12 . LWSS contour plots, deployment area of unbranched domains, instances 4–6. ....	88
Figure 3.13 . LWSS contour plots, entire area of unbranched fluid domains, instances 1–3. ....	89
Figure 3.14 . LWSS contour plots, entire area of unbranched fluid domains, instances 4–6. ....	90

Figure 3.15 . Radial gradient of velocity and shear strain rate .....	91
Figure 3.16 . Velocity magnitudes along a radial path. ....	92
Figure 3.17 . Drag force comparison in a unbranched fluid domain.....	93
Figure 3.18 . LWSS distribution in branched fluid domains.....	95
Figure 3.19 . Drag force comparison of the scaffolds in branched domains.....	96
Figure 3.20 . LWSS contour plots, deployment area of branched domains, instances 1–3.....	97
Figure 3.21 . LWSS contour plots, deployment area of branched domains, instances 4–5.....	98
Figure 3.22 . LWSS contour plots, entire area of branched fluid domains, time instances 1–3.....	99
Figure 3.23 . LWSS contour plots, entire area of branched fluid domains, time instances 4–6.....	100
Figure 3.24 . Flow rate comparison of proximal, distal and main branches.....	101
Figure 3.25 . Mean absolute flow deviation from a healthy branched vessel. ....	102
Figure 3.26 . Temporal average values of hemodynamic indicators. ....	103
Figure 3.27 . LWSS in the deployment area of cases 1–8.....	105
Figure 3.28 . LWSS in the entire fluid domains of case 1–8. ....	106
Figure 3.29 . Drag Force Comparison, cases 1–8. ....	107
Figure 3.30 . Proximal branch to inlet flow rate ratio, cases 1–8. ....	108
Figure 3.31 . Distal branch to inlet flow rate ratio, cases 1–8.....	109
Figure 3.32 . Main branch to inlet flow rate ratio, cases 1–8.....	110
Figure 3.33 . Mean absolute flow deviation. ....	111
Figure 3.34 . Temporal average values of hemodynamic indicators, cases 1–8. ....	111
Figure 3.35 . Temporal distribution of the mean LWSS ratios, cases 1–8.....	112
Figure 3.36 . Temporal distribution of mean drag force, cases 1–8.....	113
Figure 3.37 . Temporal mean flow ratios, cases 1–8.....	114
<b>Chapter 4.....</b>	<b>117</b>
Figure 4.1 . Stress-strain curve of a shape memory alloy.....	120
Figure 4.2 . Heat transfer setup model.....	122
Figure 4.3 . Cross-sectional overview of the mock-rod assembly.....	125
Figure 4.4 . Fin analysis of the heat transfer assembly. ....	129
Figure 4.5 . Thermal resistance network at the top section of mock-rod assembly.....	131
Figure 4.6 . Temperature distribution along walls of mock vessel. ....	134
Figure 4.7 . Temperature distribution along heat transfer (HT) rod. ....	135
Figure 4.8 . Temperature distribution along walls of mock vessel, high temperature input.....	136

Figure 4.9 . Geometry of the 3D thermal analysis model. ....	138
Figure 4.10 . Discretised mock-rod domain. ....	139
Figure 4.11 . Temperature distribution in the axial direction of the rod. ....	140
Figure 4.12 . Heat flux in the mock-rod assembly. ....	141
Figure 4.13 . Temperature distribution along internal walls of mock vessel. ....	142
Figure 4.14 . Temperature distribution in the simplified RRR. ....	143
Figure 4.15 . FEA model of the mock-rod assembly in a fluid chamber. ....	144
Figure 4.16 . Discretization of the fluid solid domain for conjugate heat transfer. ....	147
Figure 4.17 . Convergence plots of the conjugate heat transfer analysis. ....	148
Figure 4.18 . Temperature distribution along the rod, conjugate heat transfer. ....	149
Figure 4.19 . Velocity profile at the horizontal cross-section of the fluid chamber. ....	150
Figure 4.20 . Velocity profile at the vertical cross-section of the fluid chamber. ....	151
Figure 4.21 . Temperature on mock vessel internal walls, conjugate heat transfer. ....	152
Figure 4.22 . Temperature on mock vessel external walls, conjugate heat transfer. ....	153
Figure 4.23 . Temperature distribution in the RRR, conjugate heat transfer. ....	154
Figure 4.24 . Heat transfer setup. ....	155
Figure 4.25 . Temperature of the external surface of mock vessel, base. ....	156
Figure 4.26 . Temperature of the external surface of mock vessel, deployment area. ....	157
Figure 4.27 . <i>In vitro</i> thermal expansion of the RRR. ....	158
Figure 4.28 . Free expansion of the RRR under heat stimuli. ....	159
Figure 4.29 . Average external diameter of RRR vs. temperate. ....	159
Figure 4.30 . Actuation force measurement setup. ....	160
Figure 4.31 . Temperature distribution on the heating plate and RRR. ....	163
Figure 4.32 . Expansion forces of thermal actuation. ....	164
Figure 4.33 . Electro-thermal actuation of the RRR. ....	166
Figure 4.34 . Geometry of the electro-thermal analysis, deployment area. ....	170
Figure 4.35 . Discretization of the fluid solid domain, electro-thermal analysis. ....	172
Figure 4.36 . Convergence plots of electro-thermal analysis. ....	173
Figure 4.37 . Temperature distribution in RRR, electro-thermal analysis. ....	174
Figure 4.38 . Parametric study of electro-thermal analysis. ....	174
Figure 4.39 . Shear thinning effect of blood, electro-thermal analysis. ....	175



# List of Tables



<b>Chapter 1</b> .....	<b>1</b>
Table 1.1 . Mechanical properties of common stent materials.....	18
Table 1.2 . Common materials used for fabrication of stents. ....	21
Table 1.3 . Common stent surface enhancement strategies.....	30
<b>Chapter 2</b> .....	<b>41</b>
Table 2.1 . Material and geometrical characteristics of a typical BE stent and RRR.....	50
Table 2.2 . Surface roughness measurement parameters and values. ....	63
Table 2.3 . Properties of RRR and commercial stent samples for compression test. ....	67
<b>Chapter 3</b> .....	<b>71</b>
Table 3.1 . Material and geometrical characteristics of the three luminal supports. ....	78
Table 3.2 . Dimensional configurations of the fluid domain for sensitivity study. ....	81
Table 3.3 . Drag and withholding forces comparison in an unbranched fluid domain. ....	94
<b>Chapter 4</b> .....	<b>117</b>
Table 4.1 . Geometrical and material properties of the mock-rod assembly. ....	123
Table 4.2 . Vertical expansion of components in heat-induced actuation setup. ....	162
Table 4.3 . Material properties of blood and parylene-C.....	167